Study of surface plasma-wave reflectance and roughness-induced scattering in silver foils

S. O. Sari,* D. K. Cohen,† and K. D. Scherkoske‡
Optical Sciences Center, University of Arizona, Tucson, Arizona 85721
(Received 10 September 1979)

The results of an experimental investigation of both scattering and reflectance of roughened silver foils are described. Roughness has been induced by use of calcium fluoride on glass or of random dispersions of small spheres on glass onto which opaque silver layers have been evaporated. A detailed comparison of the wavelength location of the experimental surface-plasma resonance has been made to scattering calculations including second-order self-energy corrections to the surface-plasmon dispersion relation. Self-consistent roughness parameters have been obtained from such an analysis, although limitations in the present theory are emphasized. Remarks are made on depolarization scattering.

I. INTRODUCTION

The study of light excitations on rough metal surfaces has been the subject of repeated attention over several decades.[1] This sensitive optical probe of scattering and absorptive properties has proved to be a useful tool not only for extracting basic new surface information, but also for explaining effects of practical importance.[2] However, in these efforts it is only comparatively recently that experimental and accompanying theoretical progress has evolved to a degree where truly quantitative comparisons of measurements can be made to calculations. Thus, in an effort to utilize developments in scattering analysis occurring in the past few years,[3-6] we have made a systematic, new experimental study of roughened silver which we wish to summarize here. Several investigations of both electron-induced[7] and light-induced[8] surface-plasmon reradiation have appeared previously; yet rather than review this history, we emphasize only a few of the efforts which have served as a fruitful guide to us in this work. This includes a number of optical-roughness investigations[9-11] of normally incident light on metal surfaces.

Our present study of rough silver includes consistent scattering and reflectance measurements as well as examination of second-order roughness corrections to the surface-plasmon dispersion relation, following a recent calculation.[12] First-order corrections leading to splitting of the surface-plasmon absorption have been observed previously in anomalous reflectance spectra in potassium,[13] but have tentatively been interpreted only recently.[14] The appearance of a first-order splitting is dependent upon a preferred roughness wave vector which has not been a characteristic of the silver foils employed in this study. As part of our discussion, we note that lowest-order scattering theories, as they are presently formulated, have limitations in reproducing details of effects which seem characteristically to be of higher order. This includes macroscopic roughness corrections of evaporated silver on latex-sphere roughened surfaces and features of depolarization scattering. Perhaps as a related point the extent to which nonlocal or anomalous skin effects can contribute to silver reflectance seems only partially explored, although such corrections to the reflectance are apparently small in the visible and near-infrared frequency regions.[15]

As a preface to our remarks, it is useful to recall some simple features of surface-plasmon behavior. To do this we consider plane-wave solutions of Maxwell's equations at an interface bounded on one side ($z>0$) by vacuum and on the other ($z<0$) by a metal of dielectric constant ϵ. Consider bounded solutions of the displacement vector of the form $\overline{D}=\overline{D}_0 e^{i\vec{K}\cdot\vec{R}} e^{-pz}$ for $z>0$ and $\overline{D}=\overline{D}_0 e^{i\vec{K}\cdot\vec{R}} e^{+qz}$ for $z<0$, where $p^2=K^2-(\omega/c)^2$ and $q^2=K^2-\epsilon(\omega/c)^2$. Matching interfacial boundary conditions yield the usual surface-plasma wave dispersion relation

$$K^2=\frac{\epsilon}{\epsilon+1}\left(\frac{\omega}{c}\right)^2, \tag{1.1}$$

where we assume ϵ real. If we now take ϵ equal to $\epsilon_0-\omega_p^2/\omega^2$, we obtain

$$\frac{c^2K^2}{\omega^2}=1+\frac{\omega^2(\omega_{sp}/\omega_p)^2}{\omega_{sp}^2-\omega^2}, \tag{1.2}$$

where $\omega_{sp}=\omega_p/(1+\epsilon_0)^{1/2}$. The pole in this dispersion relation occurs at the surface-plasma resonance frequency. Moreover, in the region between ω_{sp} and $\omega_p/\epsilon_0^{1/2}$ no surface modes can be excited. This is just a "restray" region very similar to that occurring for lattice waves, that is, a frequency gap where roughness excitation *in the metal* is not possible. The importance of this feature has been described in a slightly

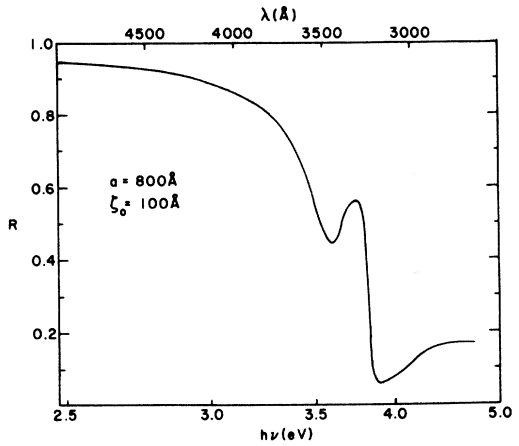

FIG. 1. Reflectance near the screened plasma edge of a roughened silver metal surface showing the resonant surface-plasma wave absorptance dip near the energy $\hbar\omega$ for which $\epsilon_R(\omega) \approx -1$. Roughness parameters for this example are rms height $\zeta_0 = 100$ Å and correlation width $a = 800$ Å. The rise in the reflectance in the region for $-1 < \epsilon < 0$ may be interpreted as a "roughness restray" region in which no roughness *absorption* is possible.

different context with regard to scattering from inhomogeneous composites,[16] but not in its present form. It explains the rise in metal reflectance in the region $0 > \epsilon > -1$ just beyond the surface-plasma resonance at $\epsilon = -1$ in a free-electron metal and just before the bulk plasma onset ($\epsilon = 0$) is reached. For positive ϵ, roughness absorption is again possible, although not resonantly. These features are qualitatively observed in most roughness reflectance spectra such as illustrated in Fig. 1.

The plan of this paper is as follows: We first summarize some of the scattering results to be used in our analysis (Sec. II), give remarks on experimental procedure in Sec. III, and explain the detailed comparison of reflectance measurements to numerology of calculations in Sec. IV. In Sec. V we approach the problem of roughness-induced angular scattering and conclude with remarks in Sec. VI.

II. ASSUMPTIONS AND RESULTS OF SCATTERING THEORIES

To obtain the analytic results used in our experimental analysis requires solutions of Maxwell's equations at an interface between a metal or dielectric and vacuum. A common approach in the treatment of this problem has been to consider the interface as flat in the lowest order and to take roughness as a perturbation. In a calculation to first order, we can define $\vec{K}$ as a two-dimensional surface wave vector in the interfacial plane. Then for wave vectors such that $|\vec{K}| = K < \omega/c = k_0$, we obtain back scattering out of the metal. On the other hand, if $K > k_0$, then the normal propagation vector of the scattered wave is imaginary, and this wave is confined to the metal. In that case, the usual damping processes in the metal will attenuate the interfacial wave in such a way that the roughness interaction will lead to an absorptive loss channel.

A perturbative method for rough surface scattering has been examined by a number of authors both classically and quantum mechanically. A quantum field theoretic treatment is, of course, the only way to properly characterize elementary excitations and thus has some claim to elegance. Yet the classical approaches used yield essentially the same final results and are preferable from the point of view of ready utility. Thus we have confined ourselves to these latter techniques. Perhaps the simplest classical approach is the Raleigh-Fano method used by Celli, Marvin, and Toigo[5] to obtain solutions to the perturbed boundary problem. This procedure depends on matching electric and magnetic fields across the perturbed interface yielding the Fresnel coefficients in lowest order. In next higher order the calculation yields s- and p-wave scattering cross sections and resonant p-wave metal absorption for ϵ_R in the neighborhood $\lesssim -1$. Here, for s-(p-) wave scattering the electric vector $\vec{E}$ is polarized normal to (or in) the scattering plane. The dielectric function ϵ is defined as $\epsilon_R + i\epsilon_I$. Yet another approach to lowest-order roughness scattering is a classical Green's function method previously developed by two theoretical groups.[3,4] For our purposes it is helpful to present some of the conclusions obtained from this approach in a simple form in order to form a basis for our experimental comparison.

To do this, define the unperturbed interface such that for $z > 0$, $\epsilon(z) = 1$ and for $z < 0$, $\epsilon(z) = \epsilon$. Let $\vec{P}_s(\vec{r})$ be the perturbed interfacial polarization due to two-dimensional surface topography variations described by

$$z = \zeta(\vec{R}) = \zeta(x, y) = \sum_K \zeta_K e^{i\vec{K}\cdot\vec{R}} .$$

Then, using the Hertz potential of Ref. 3, we may rewrite Maxwell's equations as

$$\nabla^2\vec{Z}(\vec{r}) + \epsilon(z)k_0^2\vec{Z}(\vec{r}) = -\frac{4\pi\vec{P}_s(\vec{r})}{\epsilon(z)}, \tag{2.1}$$

where

$$\vec{E} = \vec{\nabla}(\vec{\nabla}\cdot\vec{Z}) + \epsilon(z)k_0^2\vec{Z},$$
$$\vec{B} = -i\epsilon(z)k_0(\vec{\nabla}\times\vec{Z}), \tag{2.2}$$

and the vector and scalar potentials are $\vec{A} = -i\epsilon(z)k_0\vec{Z}$ and $\phi = -\vec{\nabla}\cdot\vec{Z}$. For simplicity we choose the Kth Fourier component of the surface corrugations to be along the y direction. Then for this component

$$\vec{P}_s(\vec{r}) = P_{xK}(z)e^{iKy}\hat{x} + P_{yK}(z)e^{iKy}\hat{y} + P_{zK}(z)e^{iKy}\hat{z}\,. \quad (2.3)$$

The Green's-function tensor for this problem solves the equation

$$\nabla^2\overleftrightarrow{G}(rr') + \epsilon(z)k_0^2\overleftrightarrow{G}(rr') = \overleftrightarrow{I}\delta(\vec{r}-\vec{r}')\,,$$

where $\overleftrightarrow{I}$ is the 3×3 unit matrix. In the z direction for the Kth Fourier component, we have

$$\frac{\partial^2\overleftrightarrow{G}}{\partial z^2}(zz') + [\epsilon(z)k_0^2 - K^2]\overleftrightarrow{G}(zz') = \overleftrightarrow{I}\delta(z-z')\,, \quad (2.4)$$

where

$$\overleftrightarrow{G}(rr') = e^{iK(y-y')}\overleftrightarrow{G}(zz')\,.$$

Solutions may be obtained for the tensor components of $\overleftrightarrow{G}(zz')$ by writing the Kth Fourier component of $\vec{Z}$ as

$$\vec{Z}_K(z) = -4\pi\int dz'\overleftrightarrow{G}(zz')\cdot\vec{P}_s(z')/\epsilon(z')\,, \quad (2.5)$$

and by matching the Kth Fourier scattering components of electric and magnetic fields across the perturbed interface, according to Eq. (2.2).

The results of these boundary matching techniques yield Green's-function tensor components very nearly the same as those tabulated by Refs. 3 and 4. In our calculations we have assumed a tensor in block diagonal form such that $G_{xy} = G_{yx} = G_{xz} = G_{zx} = 0$. Note also that $G_{yz} = G_{zy}$. However, we find in our procedure that an arbitrariness exists in the determination of the tensor components and that, in addition, we can obtain a form for $\overleftrightarrow{G}$ which is fully diagonal. This form contains essentially the same information content as the block diagonal $\overleftrightarrow{G}$.

It is now useful to write the perturbed interfacial polarization $\vec{P}_s(\vec{r})$ in terms of the surface roughness. To do this we write

$$\vec{P}_s(\vec{r}) = \frac{\epsilon-1}{4\pi}[\Theta(z) - \Theta(z-\zeta(\vec{R}))]\vec{E}\,, \quad (2.6)$$

where $\vec{E}$ is the transmitted electric field in the metal and $\Theta(z)$ is the unit positive step function. Then

$$\vec{P}_K(z) = (1/L^2)\int d\vec{R}\, e^{-i\vec{K}\cdot\vec{R}}\,\vec{P}_s(\vec{r})$$

and

$$\vec{P}_K = \int dz'\,\vec{P}_K(z')$$

so for small[17] surface perturbations we obtain

$$\vec{P}_K = \frac{\epsilon-1}{4\pi}\vec{E}\zeta_K\,, \quad (2.7)$$

where

$$\zeta_K = (1/L^2)\int dR\, e^{-i\vec{K}\cdot\vec{R}}\zeta(\vec{R}) = (1/L)\int dy\, e^{iKy}\zeta(y)$$

under the previous assumption of $\vec{K}\parallel\hat{y}$. The length L is our box normalization parameter.

The Kth Fourier component of the scattered fields may now be written from results of calculations. In the case of s-wave scattering

$$\vec{E}_K = \begin{cases} \dfrac{4\pi k_0^2 i P_{xK}e^{i\alpha z}e^{iKy}\hat{x}}{\gamma+\alpha} & (z>0)\,, \\ \dfrac{4\pi k_0^2 i P_{xK}e^{-i\gamma z}e^{iKy}\hat{x}}{\gamma+\alpha} & (z<0)\,. \end{cases} \quad (2.8)$$

For p-wave scattering

$$\vec{E}_K = \begin{cases} \dfrac{4\pi i(\gamma P_{yK} - KP_{zK})e^{i\alpha z}e^{iKy}(\alpha\hat{y} - K\hat{z})}{\epsilon\alpha+\gamma} & (z>0)\,, \\ \dfrac{4\pi i(\alpha P_{yK} + K/\epsilon P_{zK})e^{-i\gamma z}e^{iKy}(\gamma\hat{y} + K\hat{z})}{\epsilon\alpha+\gamma} & (z<0)\,, \end{cases} \quad (2.9)$$

where $\alpha^2 = k_0^2 - K^2$ and $\gamma^2 = \epsilon k_0^2 - K^2$. These expressions are in agreement with the scalar Green's-function method of Hunderi[9] and Beaglehole in which the effect of a rough surface is approximated by utilizing an inhomogeneous scattering layer between ordinary metal and vacuum and then matching boundary fields between the layers.

The differential scattering rates out of the metal are calculated by determining the power scattered into an element of surface K space, d^2K, and subsequently normalizing by the incident intensity. Using Eqs. (2.7) through (2.9) and taking $P_{zK} = 0$, we obtain the differential, diffuse s- and p-wave reflectance for normally-incident, polarized light which may be expressed as

$$\frac{1}{R}\frac{dR^s}{d\Omega} = \frac{k_0^4L^2|\zeta_K|^2\cos^2\theta|\sqrt{\epsilon}+1|^2}{\pi^2|\cos\theta + (\epsilon-\sin^2\theta)^{1/2}|^2}\,, \quad (2.10)$$

$$\frac{1}{R}\frac{dR^p}{d\Omega} = \frac{k_0^4L^2|\zeta_K|^2\cos^2\theta|\sqrt{\epsilon}+1|^2|(\epsilon-\sin^2\theta)^{1/2}|^2}{\pi^2|\epsilon\cos\theta + (\epsilon-\sin^2\theta)^{1/2}|^2}\,. \quad (2.11)$$

These expressions have been further normalized by the normal-incidence Fresnel coefficient $R = |1-\epsilon^{1/2}|^2/|1+\epsilon^{1/2}|^2$, where ϵ is the complex dielectric function defined previously.

The surface-plasma wave contribution to the reflectance is obtained from the Joule loss due to scattering into the metal. The reflectance change

due to this mechanism is given by the ratio of the power dissipated per unit area in the metal surface region to the power incident per unit area onto the metal surface. Carrying out these calculations using Eq. (2.7) and E_K ($z<0$) from Eq. (2.9), we obtain for normally incident unpolarized light that

$$\Delta R_{SP} = \epsilon_I k_0 |\sqrt{\epsilon}-1|^2 \sum_K |\zeta_K|^2 \frac{|\gamma|^2+K^2}{\mathrm{Im}\gamma} \frac{|\alpha|^2}{|\epsilon\alpha+\gamma|^2}. \tag{2.12}$$

The largest contributions to the reflectance in this roughness scattering theory come from those wave vectors for which the denominator $|\epsilon\alpha+\gamma|^2$ is small. To explicitly show the pole in this expression, rewrite it as

$$\frac{|\epsilon\alpha-\gamma|^2}{|\epsilon^2\alpha^2-\gamma^2|^2} \propto \frac{1}{(K^2-K_s^2)^2+\Gamma^2}. \tag{2.13}$$

This defines a surface-plasmon wave vector as

$$K_s^2 = \mathrm{Re}\left(\frac{\epsilon}{\epsilon+1}\right)k_0^2, \tag{2.14}$$

which is a slight generalization of Eq. (1.1). The damping width $\Gamma = k_0^2 \mathrm{Im}\epsilon/(\epsilon+1)$. If $\zeta(\vec{R})$ is the roughness topography function introduced earlier, then the power spectrum of roughness fluctuations $|\zeta_K|^2$ is just given by the Fourier transform of the roughness correlation function $\langle\zeta(\vec{R})\zeta(\vec{R}+\vec{\rho})\rangle$. Thus, if we assume Gaussian correlations as we have done exclusively in this paper, we have

$$\langle\zeta(\vec{R})\zeta(\vec{R}+\vec{\rho})\rangle = \zeta_0^2 e^{-\rho^2/a^2}$$

and the scattering and absorption may be calculated in terms of the parameters ζ_0 and a. The surface-plasmon reflectance change given by Eq. (2.12) in the limit of small damping ($\epsilon_I \to 0$) reduces to a simple form of

$$\Delta R_{SP} = \pi\zeta_0^2 a^2 k_0^4 \exp\left[-\frac{k_0^2 a^2}{4}\left(\frac{\epsilon_R}{\epsilon_R+1}\right)\right] \times \frac{\epsilon_R^2}{[-(\epsilon_R+1)]^{5/2}}\Theta(-(1+\epsilon_R)). \tag{2.15}$$

The experimental results to be discussed have been compared using numerical analysis to the expressions (2.12) and Eqs. (2.10) and (2.11) in the case of scattering into the air. The metal reflectance in lowest order is reduced by the scattering both into and out of the metal.

To get an estimate of the relative importance of these quantities we have numerically calculated the spectral dependence expected for the integrated s- and p-wave scattering $\Delta R^{s,p} = \int d\Omega\,(dR^{s,p}/d\Omega)$, as well as the surface-plasma wave contribution ΔR_{SP} to the reflectance of silver, using known optical constants for this metal.[18] These results are shown in Fig. 2 for the rms height parameter ζ_0 and the correlation width a of 85 Å and 1000 Å, respectively. It is evident that the vacuum scattering has far less wavelength dependence than the surface wave scattering into the metal which peaks for $\epsilon_R \sim -1$ as expected. Moreover, near the resonance peak the contribution to the difference reflectance of the surface-plasma wave component ΔR_{SP} is much larger than either of the scattered components

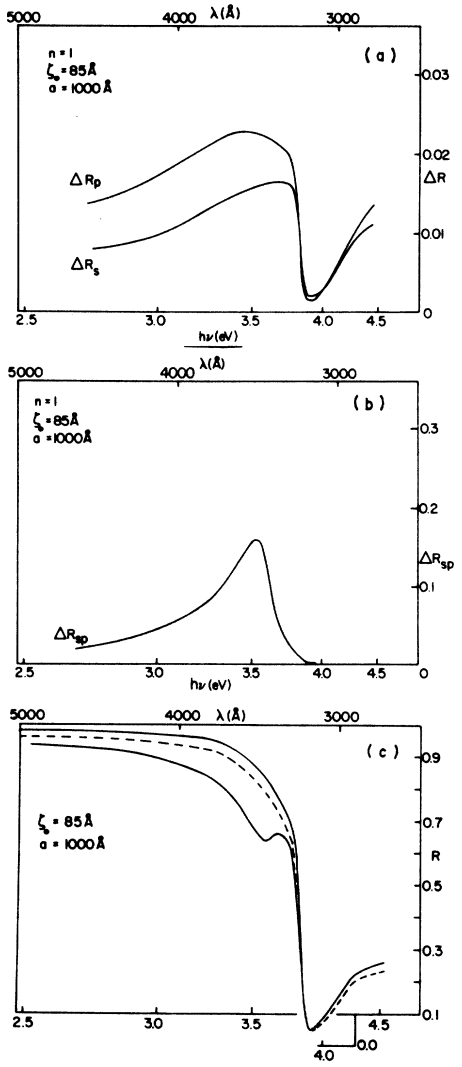

FIG. 2. Composite illustrations of calculations of: (a) integrated polarized s- and p-wave reflectance changes due to back scattering out of silver metal, (b) contribution to absorptance of surface-plasma wave scattering into the metal, and (c) contributed changes to the smooth-surface reflectance due to both these scattering contributions yielding a net rough-surface reflectance for roughness parameters $\zeta_0 = 85$ Å and $a = 1000$ Å.

ΔR^s or ΔR^p or of the sum. The contribution of each of these components is shown in the illustration of the reflectance of rough silver compared to the smooth metal surface. We have omitted "final-states" effects[19] which are one means of estimating multiple scattering corrections, since we wish to emphasize roughness changes which are small.

A significant emphasis of this paper is on the modified form of the surface-plasmon dispersion relation Eq. (2.14), including second-order scattering corrections as calculated by Toigo, Celli, Marvin, and Hill[12] and by Maradudin and Zierau,[20] which we have included in the present experimental analysis. We have used the Raleigh-Fano method to calculate this correction, following the first reference above, and have checked that this calculation agrees with the results of the second set of authors.

The resonant denominator $\gamma+\epsilon\alpha$ in the surface-plasmon reflectance ΔR_{SP} is replaced in this case by

$$\gamma+\epsilon\alpha-(\epsilon+1)^2\sum_{K'}\frac{|\zeta_{K-K'}|^2(KK'-\alpha\gamma')(KK'-\alpha'\gamma)}{\gamma'+\epsilon\alpha'}. \tag{2.16}$$

Setting the real part of this expression equal to zero gives the surface-plasmon dispersion relation including second-order scattering corrections. For the purposes of numerical calculation to be described below, the form of Eq. (2.16) may be rewritten in more concise form as

$$K_s^2=\mathrm{Re}\left(\frac{\epsilon}{\epsilon+1}\right)k_0^2+\Sigma\ . \tag{2.17}$$

The term Σ is to be viewed as a correction to the zeroth-order dispersion relation. Under the assumption of Gaussian surface correlations, one may express Σ as

$$\Sigma=\frac{\zeta_0^2a^2\epsilon^2e^{-K^2a^2/4}}{(\epsilon+1)^2}\int_0^\infty\frac{dK'K'\alpha\alpha'\,e^{-K'^2a^2/4}}{K'^2-K_s^2-i\Gamma}\left[\left(\epsilon^2\alpha^2\alpha'^2+\frac{K^2K'^2}{2}\right)I_0\left(\frac{KK'a^2}{2}\right)+2\epsilon\alpha\alpha'KK'I_1\left(\frac{KK'a^2}{2}\right)+\frac{K^2K'^2}{2}I_2\left(\frac{KK'a^2}{2}\right)\right]. \tag{2.18}$$

In this expression the functions $I_n(x)$ are modified Bessel functions of the first kind. Moreover, as a matter of simplification we have taken $\epsilon\alpha\approx-\gamma$ where this can be taken without introducing a pole. This means the above expression is only approximate, but since the important contributions to the integral occur where the condition $\epsilon\alpha\approx-\gamma$ is already satisfied, the error introduced is expected to be of higher order. Our method of treatment of this somewhat cumbersome correction integral is described in Sec. IV.

It should be noted that analogous first-order roughness corrections to the surface-plasmon resonance may be obtained for surfaces containing partial order or, in other terms, any preferred surface scattering wave vectors. This can lead to multicomponent resonance structure,[12-14] but does not occur for stochastic surfaces having no preferred wave vector.

III. EXPERIMENTAL CONSIDERATIONS

Reflectance measurements reported in this paper were obtained by a difference technique to compare rough Ag to smooth Al using a difference reflectometer described previously.[21] The Al absolute reflectance was calculated from known optical constants,[22] and the smooth Ag reflectance measured in this manner could be compared to previous smooth Ag measurements[18] for calibration purposes. Absolute metal reflectance measurements are weakly dependent on sample preparation even for smooth silver samples, but consistent reflectance values to well within 1% could typically be obtained.

Concurrent measurement of surface optical scattering distributions was undertaken with a laser scattering configuration arranged as follows: A chopped p- or s-polarized Ar^+ or He-Ne beam was reflected normally from the rough Ag surface examined. Scattered light in a 4×10^{-3} sr cone was collected at 5° intervals between 15° and 90°. To ensure normalization independent of incident light fluctuations the synchronously detected scattered signal was electronically divided by another synchronous signal picked off from a portion of the input beam. The absolute magnitude of the measured polarized scattering cross section $(1/R)(dR^{s,p}/d\Omega)$ was dependent on an initial normalization of the incident beam intensity. Because of various systematic errors, these cross sections have an estimated accuracy of ~10%.

Rough silver foils utilized in this study were prepared using various techniques. Uniform roughness (correlation length $a\ll\lambda$) could be obtained by evaporating an opaque layer of silver (0.5 μm) onto 0.05- μm to 0.3-μm-thick CaF_2 underlayers on glass substrates. Using this procedure we found that by varying the CaF_2 thickness various degrees of roughness could be ob-

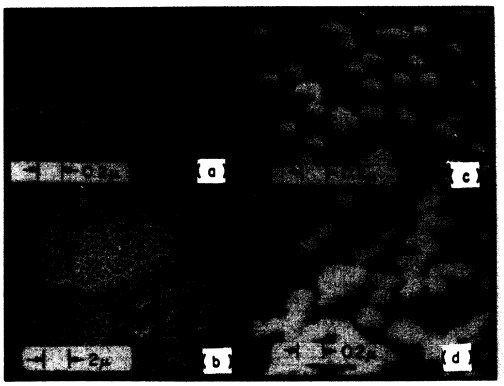

FIG. 3. Scanning electron micrographs of roughened surfaces showing: (a) Calcium fluoride roughened silver having surface correlation lengths in the range 800–1000 Å. (b) Silver surface having both rough and wavy components (i.e., regions having both $a < \lambda$ and $a \gtrsim \lambda$ respectively). (c) Latex spheres (diam = 890 Å) on glass. (d) Evaporated silver on latex-sphere surfaces of preceding case (c) producing a macroscopically roughened silver surface.

tained. Surfaces of extreme roughness were prepared by evaporating Ag onto random dispersions of very small (890 Å) latex spheres on glass. Acid etching of glass or other similar procedures prior to evaporation tended to produce wavy metal surfaces ($a \gg \lambda$). However, useful experiments could be done on rough surfaces which sometimes also contained a wavy component. These surfaces exhibited both short- and long-range correlations, and we will use the terms "rough" and "wavy" further in this context. In fact, as shown in Sec. V, a small wavy component was often obtained for surfaces which were primarily uniformly rough. Examples of these various cases of roughness are illustrated in Fig. 3.

IV. CORRECTIONS TO THE SURFACE-PLASMA-WAVE DISPERSION THEORY AND DISCUSSION OF NUMERICAL COMPARISON TO REFLECTANCE EXPERIMENTS

In analyzing our roughness-induced reflectance measurements, we found it useful to consider the effect of each of several contributions to the surface-plasma wave scattering. Each of the mechanisms considered adds a correction to the location of the surface-plasmon resonance absorption. Thus, it has been our intent to compare the experimental location of the resonance position with calculations based on the roughness theory presented to see how precisely experiment and calculation agree.

In the present discussion we examine the surface-plasmon dispersion relation progressively as more detailed contributions are included in our analysis. Following Eqs. (2.14) and (1.1) and using the simple, real unscreened Drude expression $\epsilon = 1 - \omega_p^2/\omega^2$ for the dielectric function, we obtain a pole in the surface wave vector K for $\omega_{sp} = \omega_p/2^{1/2} = 9.79 \times 10^{15}$ Hz ($\omega_p = 13.85 \times 10^{15}$Hz for Ag). Including the zero-frequency d-band (and core) screening contribution gives $\omega_{sp} = \omega_p/(1+\epsilon_0)^{1/2} = 6.54 \times 10^{15}$ Hz, using $\epsilon_0 = 3.5$.[23] A slight extension is to include the frequency de-

TABLE I. Summary of corrections to the surface-plasma resonance wavelength of silver. Experiment: 3550 Å.

Contribution	$\epsilon(\omega)$	ω_{sp}	λ (Å) ($\lambda_p = 1360$ Å)	ω (10^{15} Hz)	$h\nu$ (eV)	$\Delta\lambda$	$10^{15}\,\Delta\omega$	ΔE (eV)
Bare resonance	$1-\frac{\omega_p^2}{\omega^2}$	$\omega_p/\sqrt{2}$	1924	9.79	6.32			
						920	−3.07	−2.02
Zero-frequency d-band correction	$\epsilon_0-\frac{\omega_p^2}{\omega^2}$	$\omega_p/(1+\epsilon_0)^{1/2}$	2880	6.54	4.30			
Self-consistent d-band correction	$\epsilon_d(\omega)-\frac{\omega_p^2}{\omega^2}$	$\frac{\omega_p}{[1+\epsilon_d(\omega_{sp})^{1/2}]}$	3350	5.62	3.70			
						50	−0.08	−0.05
Damping due to electron-hole excitations and interband transitions	$\epsilon_R + i\epsilon_I$		3400	5.54	3.65			
						50	−0.08	−0.06
Correlation length cutoff	$a = 800$ Å		3450	5.46	3.59			
						80	−0.12	−0.08
Self-energy correction			3530	5.34	3.51			
					Totals	1570	−4.27	−2.81

pendence of the d-band correction, which is equivalent to using the known optical dielectric function $\epsilon_R(\omega)$ in a self-consistent way to estimate the surface-plasma frequency. This yields $\omega_{sp} = 5.62 \times 10^{15}$ Hz. Making allowance for damping, resulting from both electron-hole and interband excitations, we introduce an imaginary component to ϵ and from Eq. (2.14) we obtain a dispersive form for K, having a rounded pole. A maximum value for the surface scattering wave vector K_{max} occurs at frequencies ω of approximately 5.5×10^{15} Hz. However, those wave vectors physically important in the surface wave scattering process will be considerably smaller than K_{max}. In the Gaussian correlation-length approximation, the dominant wave vectors K are of order $2/a \ll K_{max}$. The averaging over physically important wave vectors produces a further correction to the surface-plasmon reflectance minimum, as we have determined by numerical analysis of Eq. (2.12). This is also evident from examining the expression ΔR_{SP} as given by Eq. (2.15). The amount of the shift (for $a \approx 800$ Å) is approximately -0.1×10^{15} Hz on the frequency value given without this correction.[24] These contributions to the surface-plasma wave resonance are all expressed in Table I. The shape of the K vs ω dispersion relations under the conditions just described are summarized concurrently in Fig. 4.

The principal additional mechanism which we have considered is the second-order surface scattering of surface plasmons.[25] This yields a correction to the surface-plasmon dispersion relation as given in Eq. (2.17) and an additional wavelength shift in the surface wave resonance. When employed with self-consistent roughness parameters, the correction can explain a sizable fraction of the discrepancy between theory and reflectance experiments as to surface-plasma resonance location. Other possible contributions accounting for remaining discrepancies have not been included, but are presently believed to be relatively small. The wavelength redshifts produced by this plasmon scattering mechanism are of order 50 Å and have also been summarized in Table I.

Some of the details of our numerical computations will now be given. All numerics were performed on an Eclipse S200 minicomputer. To evaluate the integral Σ over K' as given in Eq. (2.18), we used Simpson's rule. In the integration it was found that the rapidly decreasing behavior of the factor $\exp(-K'^2a^2/4)$ in the integrand allowed for an upper-limit truncation at the values of K' such that the dimensionless parameter $K'/k_0 \approx 25$. The same approximate

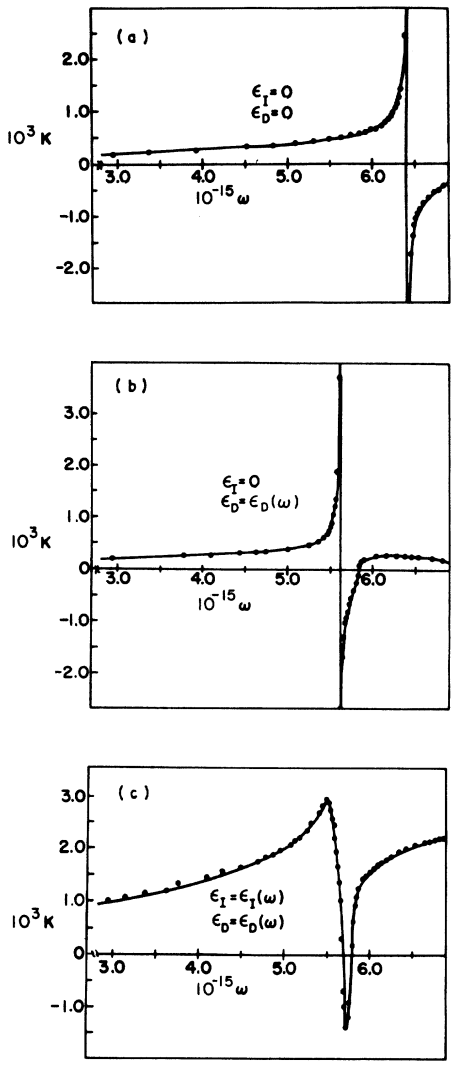

FIG. 4. Surface-plasmon dispersion curves of surface wave vector K versus photon frequency ω for progressively more detailed dielectric functions of silver. In case (a), $\epsilon = \epsilon_R$ where $\epsilon_R = 1 - \omega_p^2/\omega^2$ and the surface-plasmon pole occurs for $\omega = \omega_p/\sqrt{2}$. In case (b), damping is omitted, but $\epsilon = \epsilon_R(\omega) = \epsilon_D(\omega) - \omega_p^2/\omega^2$, so the pole is now at $\omega_{sp} = \omega_p/[1 + \epsilon_D(\omega_{sp})]^{1/3}$. In case (c) the dielectric function $\epsilon = \epsilon_R(\omega) + i\epsilon_I(\omega)$ is complex and the dispersion relation follows Eq. (2.14). Optical constants from Ref. 18 have been used in this numerical calculation.

cutoff was used for reflectance calculations involving Eq. (2.12), and the numerical values obtained in both of these cases were rather insensitive to making the upper-limit parameter either 50% larger or smaller. About 3000 intervals were taken in the integration, with about one fourth of the intervals within about one unit on either side of the critical value of K_s/k_0. A table look-up and Lagrangian interpolation was

used to obtain values for the modified Bessel functions $I_n(x)$ accurate to order 0.1%. The accuracy of our final calculation for Σ is estimated to be within a few percent.

Results of numerical evaluation of $\mathrm{Re}\Sigma$ and $\mathrm{Im}\Sigma$ for $\zeta_0 = 100$ Å and for correlation lengths of 1000 Å and 3000 Å are shown in Fig. 5. The gap seen in the two curves for the segment of the abscissa $\omega \simeq (5.7-5.7)\times 10^{15}$ Hz occurs for $\mathrm{Re}[\epsilon/(\epsilon+1)] < 0$. Since only wave vectors $K > 0$ contribute to physically allowed processes within our present formulation, cases for which $K < 0$ are omitted. The dispersion relation Eq. (2.17) corrected by $\mathrm{Re}\Sigma$ is displayed in Fig. 6 and illustrates the K vs ω region which contributes most strongly to the surface-plasma wave peak. As noted earlier, the resonance location is

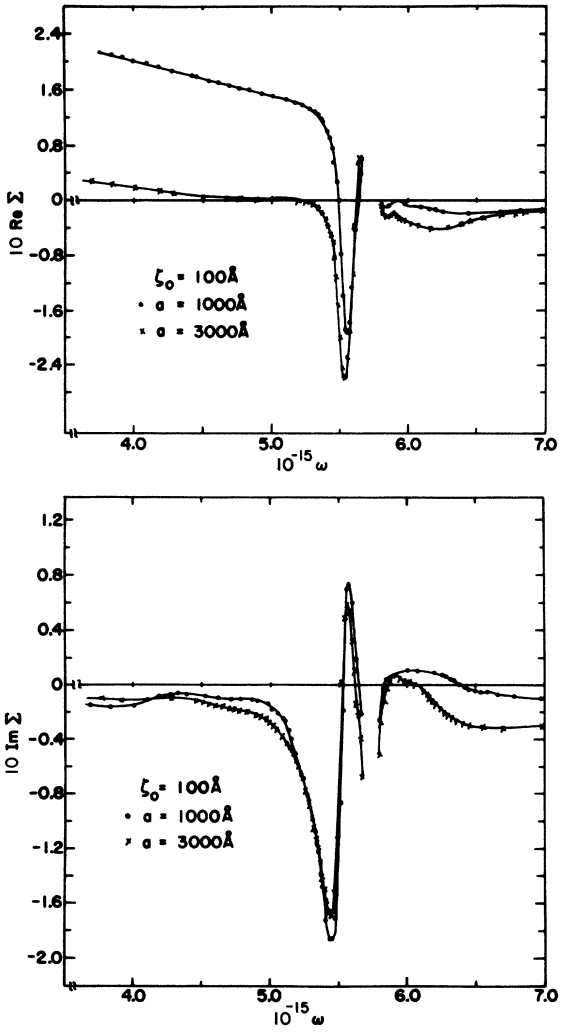

FIG. 5. Real and imaginary parts to the second-order surface plasma wave scattering correction to the dispersion relation as given by Eq. (2.18).

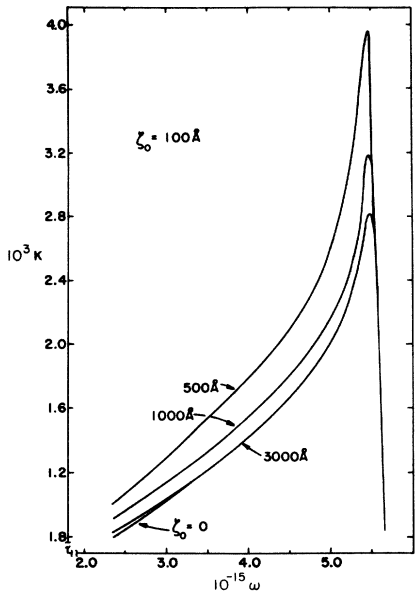

FIG. 6. Surface-plasmon dispersion relation Eq. (2.17) showing surface wave vector K versus photon frequency ω in the physically interesting region in which $K \sim 2/a$. Surface scattering corrections are included for $\zeta_0 = 100$ Å and for $a = 500$, 1000, and 3000 Å. The 3000 Å curve differs only slightly from the uncorrected curve for which $\zeta_0 = 0$ (tail shown).

down shifted in frequency for fixed surface wave vectors (0.1×10^{15} Hz for $\zeta_0 \sim 50$ Å and $a \sim 800$ Å). We remark that as $a \to \infty$ or as $\zeta_0 \to 0$ the correction term $\Sigma \to 0$, so that just the bare dispersion curve is regained.

Using these results we may compare numerical calculations to experimental reflectance line shape. The reflectivity for a stochastically roughened surface is structureless except for the central surface plasmon peak. Thus, for such surfaces it has been possible to get agreement

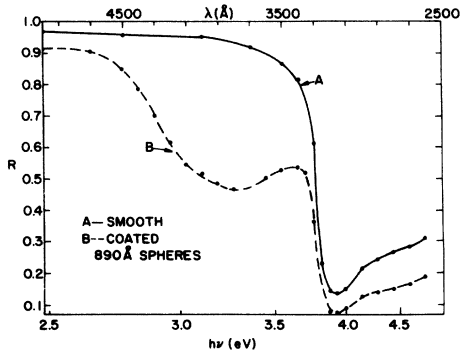

FIG. 7. Reflectance of silver evaporated on a random dispersion of 890 Å latex spheres on glass. The surface-plasma resonance in this case yields a negative step or notch in the reflectance near the screened plasma edge.

between reflectance curves and the calculations described to within about 1% for frequencies ω near the surface-plasma frequency. Partial or complete grating order results in additional surface wave structure in the reflectance as mentioned previously, but was never definitely observed in any of our present experiments.

As an extension of our results, we display Fig. 7 which was obtained for latex-sphere roughened surfaces. Here the reflectance is illustrated for a large roughness case. In this instance, it is seen that the surface-plasmon reflectance change ΔR_{SP} is no longer a peak, but rather a notch in the reflectivity. These results are perhaps more consistent with an inhomogeneous medium approach to analysis[16] rather than to a simple roughness theory.

V. DISCUSSION OF SCATTERING FROM ROUGH SURFACES

Concurrent to examining reflectance measurements, we obtained systematic numerical comparisons of angular scattering data to the scattering cross sections of Eqs. (2.10) and (2.11). Under the assumption of Gaussian correlations $|\zeta_K|^2 = \pi\zeta_0^2 a^2 e^{-K^2a^2/4}$ and the parameters ζ_0 and a could both be determined through numerical computations. The parameter pairs (ζ_0, a) were not unique, as there were a number of sets yielding

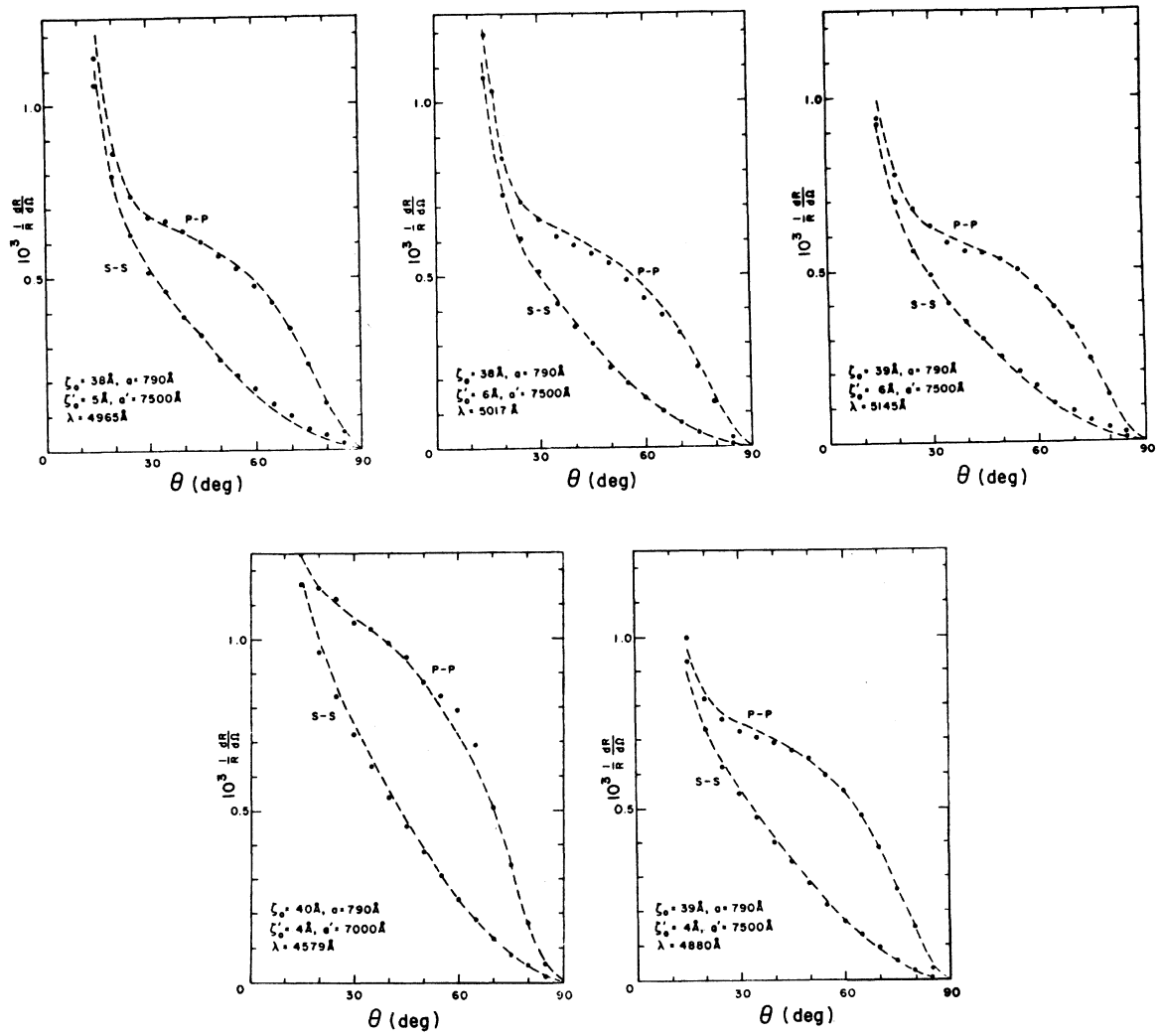

FIG. 8. Angular scattering distribution versus scattering angle for normally-incident radiation on rough silver at various Ar^+ laser wavelengths. A four-parameter fit of roughness and waviness has been used to analyze both high and low angle portions of these spectra. Since the roughness parameters obtained in these cases are nearly consistent, the scattering theory used is seen to give satisfactory results for parameters in the range shown ($0 < \zeta_0 \lesssim 50$ Å).

relative minimum least-squares comparisons to data. Thus we found several correlation lengths a in the range 800–1200 Å yielding comparable best fits with the rms height parameter ζ_0 varying simultaneously from about 50 to 40 Å. This analysis was extended, however, to calculating both the reflectance and the second-order plasma resonance correction. With these additional experimental inputs, smaller correlation length values in the range above were found to be favored along with slightly larger rms roughness heights.

In Fig. 8 we show a set of experimental curves of angular scattering distributions for various Ar^+ laser wavelengths and those parameters obtained from numerical comparison. Both rough and wavy parameters could be extracted in this procedure, assuming a Gaussian form for both these correlations. This means that four parameter comparisons were undertaken by fitting small- and large-angle scattering separately. To check this rough-wavy assumption independently we simply determined the roughness power spectra $|\zeta_K|^2$ vs $K = k_0 \sin\theta$. An example is shown in Fig. 9 for wavelengths of 6328, 5145, and 4579 Å. The silver foil in this instance was not identical to the sample yielding curves displayed in Fig. 8 but was nonetheless similar. The fact that the s- and p-wave roughness power spectra are nearly degenerate and that the power spectra determined are nearly independent of wavelength suggests that the theory used within the present limits ($\zeta_0 \lesssim 50$ Å, $a \gtrsim 800$ Å) is valid. Moreover, the shape of $|\zeta_K|^2$ versus scattering wave vectors suggests the importance of both short- and long-range correlations showing that both roughness and waviness contribute to the structure. Specifically, the long-range correlations yield a central maximum for small wave vectors K, while short-range correlation yields a rounded pedestal for larger K upon which this central peak occurs. For rougher surfaces there can be deviations. In Fig. 10, for example, the lifting of degeneracy of $|\zeta_K|^2$ with scattering wavelength is taken to indicate a limitation in the lowest-order scattering results. This suggests a possible need to extend calculations in the case in which roughness variations are larger. However, the mechanism leading to the observed deviation is here uncertain.

In the scattering distribution analyzed thus far, we have given attention to *polarized* scattering, i.e., scattering with both the incident and scattered electric vector in the scattering plane (p-p) or out of the scattering plane (s-s). It is important also to consider the cross-polarization

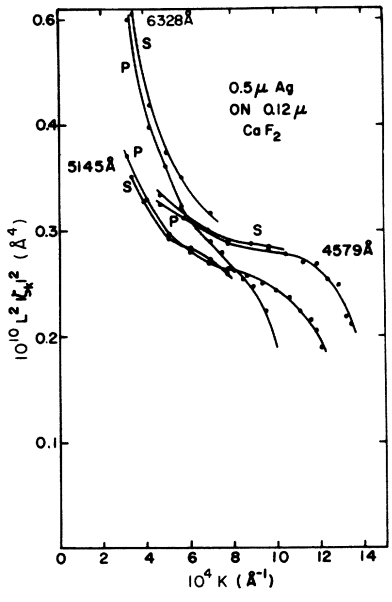

FIG. 9. Roughness power spectrum $|\zeta_K|^2$ vs $K = k_0 \sin\theta$ for a roughened silver surface similar to that examined in Fig. 8. Degeneracy of s- and p-wave scattering and of results at different wavelengths suggests validity of present theory. Shape of curve shows both short- and long-range correlations supporting the four-parameter roughness-waviness assumption discussed in the text.

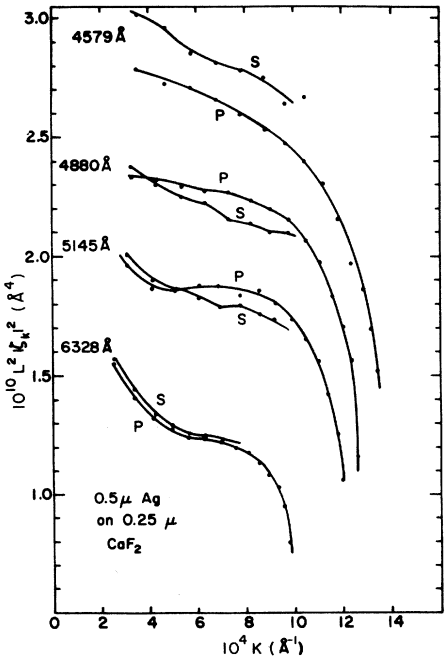

FIG. 10. Roughness spectrum $|\zeta_K|^2$ vs K for a surface having a larger roughness height parameter than in the case shown in Fig. 9.

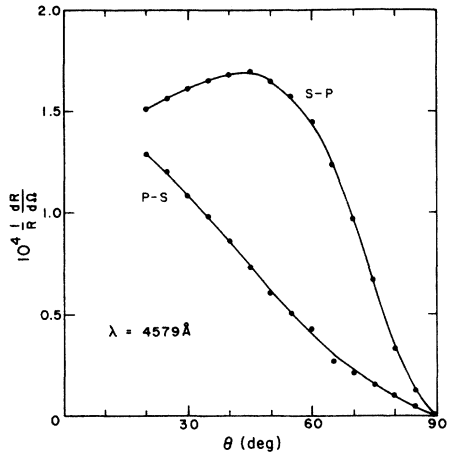

FIG. 11. Cross-polarized scattering from rough silver at $\lambda = 4579$ Å. The spectrum shown is obtained from the same sample as those given in Fig. 8.

contributions to the scattering such as that given in Fig. 11. Although polarized scattering has been extensively examined, it seems that only Beaglehole and Hunderi[9] have previously studied the presence of depolarized radiation in detail. In this case the reradiated s- and p-field distributions follow the same scattering laws as for polarized scattering. The intermediary states serving as sources for these fields can be either metal surface currents induced by the incident field or scattered electromagnetic radiation inducing polarization near the metal boundary. For simplicity, let us deal with both of these entities as surface currents which, in the case of depolarization scattering, must be treated in modified form. Because of scattering by the metal surface irregularities, these induced currents will have perturbed, scattered spatial components perpendicular to the incident field and can thus reradiate a cross-polarized field. The perpendicular current components will be either normal to the metal surface or in the surface plane. The currents normal to the surface will alter the p-wave reradiation. The s-wave radiation will be unaltered by this mechanism, since normal currents do not radiate s waves.

These considerations will lead to an important new effect, not previously viewed as significant. If we consider the p-wave radiation cross section which we would calculate from Eqs. (2.9) and (2.11) assuming only normal currents to exist, then this angular distribution has a maximum. Assuming that $|\epsilon_R| \gg \epsilon_I$ and that $\epsilon_R < 0$, we obtain a maximum at the angle θ for which

$$\tan\theta = |\epsilon_R|^{1/4}. \tag{5.1}$$

This angle is a limiting angle, since the contribution to the scattered light by currents *in* the surface plane also produce a scattering distribution, though not an angular distribution with a maximum. If the roughness scattering induces spatial surface current components both in the surface plane and normal to the plane which are in phase, then the calculated scattering maximum

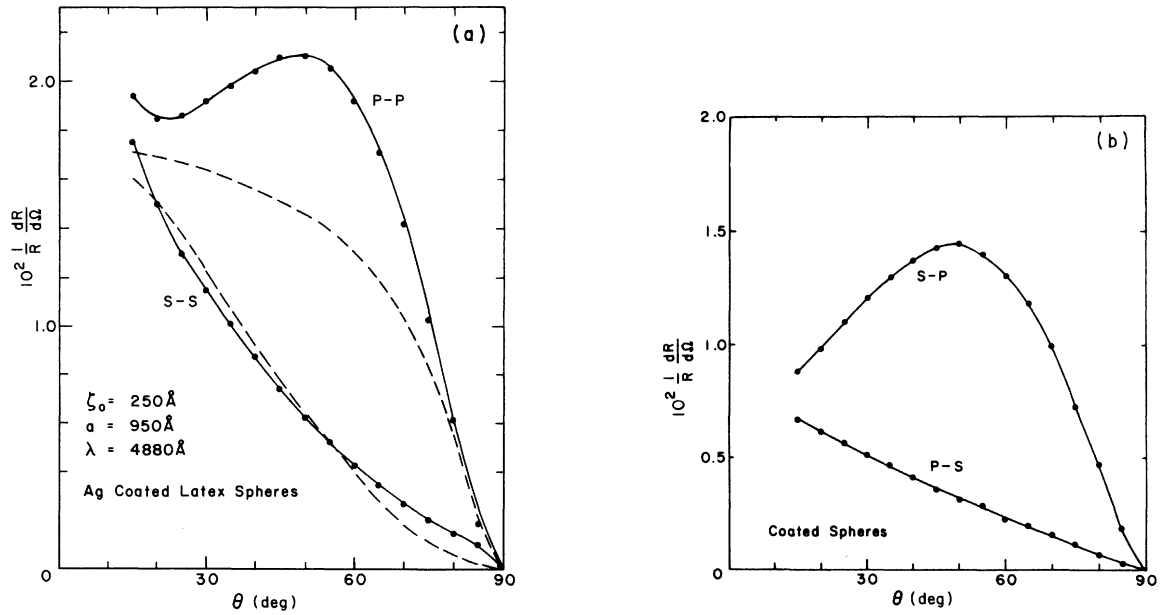

FIG. 12. Polarized p-p and s-s scattering (a) and s-p and p-s scattering (b) from a latex-sphere roughened surface. This spectrum is from the same sample as that shown in Fig. 7.

occurs at an angle between zero and the value $\tan^{-1}|\epsilon_R|^{1/4}$ given by Eq. (5.1). These remarks are consistent with the observed p-wave distribution of Fig. 11 and others observed. The existence of this maximum angle was apparently first pointed out in the numerical calculations of Beaglehole and Hunderi, who showed that very simple calculations could be used to fit their depolarization scattering curves.

Even the polarized radiation distribution from a sufficiently rough surface can be similarly modified. Returning to the case of sphere-roughened surfaces, we see in Fig. 12 that even the p-p scattering distribution has a maximum. The dashed line in this case is a calculation to the data from Eqs. (2.11) and (2.12), ignoring the normal current effect. The correlation length obtained seems rather close to a plausible value of order of the substrate sphere diameter, although the calculation in the approximation taken really only reproduces the s-wave distribution. The cross-polarized scattering for the spheres (Fig. 12) again has a strong, observed p-wave peak, as expected from perpendicular metal surface currents.

The question of inhomogeneous oxide layer corrections to the metal reflectance is taken up elsewhere.[26] However, we may make two general remarks. First, the presence of an inhomogeneous oxide reduces the metal reflectance due to scattering and absorption from this overlayer. In this respect the mechanism is similar to absorption and scattering from the rough metal itself. Second, the rough oxide scattering spectrum for a very thin covering is similar to that of the rough metal scattering.[23] However, we found that oxide residues formed on our foils had correlation lengths comparable to the optical wavelength and thus were wavy, according to our earlier nomenclature. Fortunately, from the point of view of sample preparation, rough metal scattering can, in many cases, be separated from that due to oxide, since surface oxide does not appear to form quickly.[27] In our case, silver foils examined at room temperature and stored in dry air over a period of a few days were found to remain oxide free. This was convenient for the purpose of these experiments.

VI. SUMMARIZING REMARKS

The object of this study has been to give a self-consistent experimental analysis of reflectance changes and scattering caused by roughness in silver metal surfaces. The approach is believed to be unique in an attempt to include the contribution of various mechanisms in determining the surface-plasma resonance location in the reflectance. Our study fills a useful gap between the recent theoretical treatments on this subject and some of the experimental work which is already about a decade old. Further efforts involving optical work are likely to be needed on partially disordered surfaces having a more extensive surface spectrum, on optical studies of nonlocal effects, and on electrochemically related oxide problems.

ACKNOWLEDGMENTS

We wish to thank Bruce da Costa for his capable assistance on numerous aspects of the computer analysis for this study, Tom Teska for aid in producing electron micrographs of surfaces, and Ross Potoff for his excellent sample preparation. This work was supported by the Department of Energy, Division of Materials Research under Contract No. EG-77-S-02-4381.

---

*Present address: Oregon State University, Corvallis, Oregon 97331.

†Present address: Electro-Optics Test Division, Bell Technical Operations-Textron, Tucson, Arizona 85706.

‡Present address: Department of Physics, Canisius College, Buffalo, New York 14208.

[1]See, in particular, the review articles on optical surface effects in *Advances in Chemical Physics*, edited by I. Prigogine and S. A. Rice (Wiley, New York, 1974), Vol. 27.

[2]The degradation of solar or laser mirrors via roughness are example cases. J. M. Elson, Kirtland Laboratory Technical Report No. AFWL-TR-75-210, Kirtland AFB, New Mexico, 1976 (unpublished).

[3]J. M. Elson and J. M. Bennett, Opt. Eng. 18, 116 (1979); J. M. Elson and R. H. Ritchie, Phys. Status Solidi 62, 461 (1974).

[4]A. Maradudin and D. L. Mills, Phys. Rev. B 11, 1392 (1975).

[5]V. Celli, A. Marvin, and F. Toigo, Phys. Rev. B 11, 1779 (1975).

[6]E. Kröger and E. Kretschmann, Phys.Status Solidi 76, 515 (1976).

[7]W. Steinmann, Phys. Rev. Lett. 5, 470 (1960); G. E. Jones, L. S. Cram, and E. T. Arakawa, Phys. Rev. 147, 515 (1967); T. L. Hwang, S. E. Schwarz, and R. K. Jain, Phys. Rev. Lett. 36, 379 (1976).

[8]J. Brambring and H. Raether, Phys. Rev. Lett. 15, 882 (1965); H. Morawitz and M. R. Philpott, Phys. Rev. B 10, 4863 (1974); J. Bodesheim and A. Otto, Surf. Sci. 45, 441 (1974); L. J. Cunningham and A. J. Braundmeier, Phys. Rev. B 14, 479 (1976).

[9]D. Beaglehole and O. Hunderi, Opt. Commun. 1, 101 (1969); Phys. Rev. B 2, 309 (1970); *ibid.* 321 (1970).
[10]J. G. Endriz and W. E. Spicer, Phys. Rev. B 4, 4144 (1971).
[11]S. N. Jasperson and S. E. Schnatterly, Phys. Rev. 188, 759 (1969).
[12]F. Toigo, A. Marvin, V. Celli, and N. R. Hill, Phys. Rev. B 15, 5618 (1977).
[13]R. E. Palmer and S. E. Schnatterly, Phys. Rev. B 4, 2329 (1971).
[14]E. Kretschmann, T. L. Ferrell, and J. C. Ashley, Phys. Rev. Lett. 42, 1312 (1979).
[15]H. E. Bennett, J. M. Bennett, E. J. Ashley, and R. J. Motyka, Phys. Rev. 165, 755 (1968).
[16]D. Stroud, Phys. Rev. B 19, 1783 (1979).
[17]The criterion of small in this case means not only that the surface topography height variations be $\ll\lambda$, but alo that they be $\ll\lambda/2\pi(|\epsilon_R|)^{1/2}$, the metal skin depth. Near the screened plasma edge of silver, this number is of order 200–300 Å.
[18]P. B. Johnson and R. W. Christy, Phys. Rev. B 6, 4370 (1972).
[19]Following Ritchie, this has been used by Endriz and Spicer, Ref. 10, p. 4148. It will tend to yield lower height parameters ζ_0 than use of the roughness theory without this correction.
[20]A. Maradudin and W. Zierau, Phys. Rev. B 14, 484 (1976).
[21]E. D. Huber and S. O. Sari, Rev. Sci. Instrum. 50, 438 (1979).
[22]H. J. Hagemann, W. Gudat, and C. Kunz, Report No. SR-74/7 DESY, 1974 (unpublished).
[23]See e.g., S. O. Sari and E. D. Huber, Solid State Commun. 30, 487 (1979).
[24]The approximate form for this correlation length correction to the resonance minimum is also given from calculations (cf. Fig. 4) in J. Crowell and R. H. Ritchie, J. Opt. Soc. Am. 60, 794 (1970).
[25]J. A. Bush, D. K. Cohen, K. D. Scherkoske, and S. O. Sari (unpublished).
[26]Ref. 23 and D. K. Cohen, S. O. Sari, and K. D. Scherkoske, in *Proceedings of the Conference on Non-traditional Approaches to the Solid-Electrolyte Interface*, Snowmass, Colorado, 1979, edited by T. E. Furtak, K. L. Kliewer, and D. W. Lynch (North-Holland, New York, to be published).
[27]Note, however, the possibility for spontaneous oxidation in liquids as pointed out in D. K. Cohen, S. O. Sari, and K. D. Scherkoske, in *Proceedings of the Conference on Fast Ion Transport in Solids, Lake Geneva, Wisconsin*, 1979, edited by P. Vashishta and J. N. Mundy (North-Holland, New York, 1979), pp. 189–192.

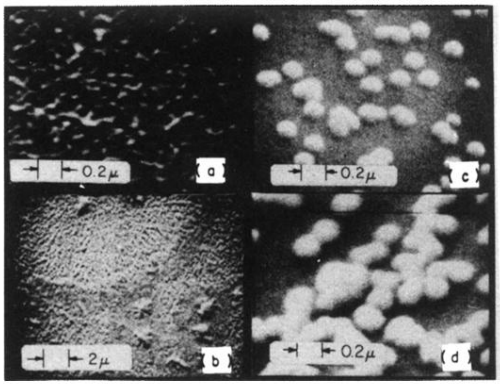

FIG. 3. Scanning electron micrographs of roughened surfaces showing: (a) Calcium fluoride roughened silver having surface correlation lengths in the range 800–1000 Å. (b) Silver surface having both rough and wavy components (i.e., regions having both $a < \lambda$ and $a \gtrsim \lambda$ respectively). (c) Latex spheres (diam = 890 Å) on glass. (d) Evaporated silver on latex-sphere surfaces of preceding case (c) producing a macroscopically roughened silver surface.